Journal of Applied Polymer Science

# Biomimetic Design of Chelating Interfaces

**Fang Tian,[1] Maxine J. Roman,[1] Eric A. Decker,[1,2] Julie M. Goddard[1]**

[1]Department of Food Science, University of Massachusetts, Amherst, Massachusetts 01003

[2]Bioactive Natural Products Research Group, Department of Biochemistry, Faculty of Science, King Abdulaziz University, P. O. Box 80203, Jeddah 21589 Saudi Arabia

Correspondence to: J. M. Goddard (E-mail: goddard@foodsci.umass.edu)

**ABSTRACT:** Siderophores are naturally occurring small molecules with metal binding constants greater than many synthetic chelators. Herein, we report a two-step process to graft a siderophore-mimetic metal chelating polymer from a polypropylene (PP) surface. Poly(methyl acrylate) was first grafted from the PP surface by photoinitiated graft polymerization, followed by the conversion into poly(hydroxamic acid) (PHA) to obtain PP-*g*-PHA films. ATR/FTIR, contact angle, SEM, and AFM were performed to characterize surface properties of films. Iron binding kinetics and the influence of pH (3.0–5.0) on the chelating ability of films were determined. PP-*g*-PHA exhibited significant iron chelating activity (~80 nmol/cm$^2$) with an equilibration time of 24 h. The materials retained 50% chelating ability at pH 3.0 compared with pH 5.0, almost double the retention of previously reported polycarboxylate chelating interfaces. By using siderophore-mimetic surface chemistry, such effective metal chelating interfaces can extend the applications of metal chelating polymers in environmental remediation, water purification, and active packaging areas. © 2014 Wiley Periodicals, Inc. J. Appl. Polym. Sci. **2015**, *132*, 41231.

**KEYWORDS:** biomimetic; packaging; photopolymerization

Received 24 February 2014; accepted 15 July 2014

**DOI: 10.1002/app.41231**

## INTRODUCTION

Metal chelating polymers have gained considerable attention in recent years due to their importance in biomedical, environmental, and biotechnology applications. Much research has been conducted on new approaches to synthesize metal chelating polymers that remove heavy metals in wastewater purification systems.[1–9] In analytical chemistry, chelating polymers bearing different functional groups have been developed for the chromatographic separation or exchanging of metal ions and metal-containing substances.[10–15] The biomedical significance of metal chelators has also been extensively exploited for applications in drug delivery,[16] iron chelation therapy,[17,18] selective inhibition of metal-containing enzymes,[18] etc. In addition, the application of interfacially chelating polymers as active packaging materials has recently been reported in which chelation by the package inhibits iron promoted oxidative degradation of nutrients, lipids, etc.[19,20]

In the interest of improving treatment options for metal chelation therapy, the biomedical field has identified a class of high metal chelating affinity, naturally derived small molecules called siderophores. Siderophores are low molecular weight metal chelators secreted by microorganisms and plants to enable solubilization and uptake of iron in iron-poor environments. One major group of siderophores contains hydroxamic acids (HAs) as the metal chelating ligands. This family of siderophores has a very high specificity and affinity to metal ions, especially ferric iron ($Fe^{3+}$), over a wide range of pH values.[21] A representative compound of this group is desferrioxamine (DFO) [Figure 1(A)], which can interact with $Fe^{3+}$ to form an iron complex with an extremely high stability constant (log $K = 30.6$).[18] DFO has been approved by FDA as a drug and is widely used in medicine for clinical treatment of patients with iron overload.[22,23]

The high specificity and affinity of the functional groups (e.g., HA) in siderophores for metal chelation has inspired researchers to design biomimetic metal chelating polymers [Figure 1(B)]. The majority of published research in this area has focused on synthesis of free macromolecules, hydrogels, and resins with biomimetic metal chelating functionality.[4,5,17,24–28] However, the ability to impart siderophore-mimetic chelating functionality to the surface of solid supports would enable significant improvements in recovery and reuse of chelating materials, and expand their societal and commercial impact (e.g., separation process for wastewater treatment, active packaging applications, etc.). Further, by manipulating only the surface chemistry, desirable bulk material properties (optical, thermo-mechanical, magnetic, and economic) can be maintained, which can further expand the application of such materials. To the best of the authors' knowledge, no research has been reported in which siderophore-mimetic functionality is introduced to the surface of a planar solid support.

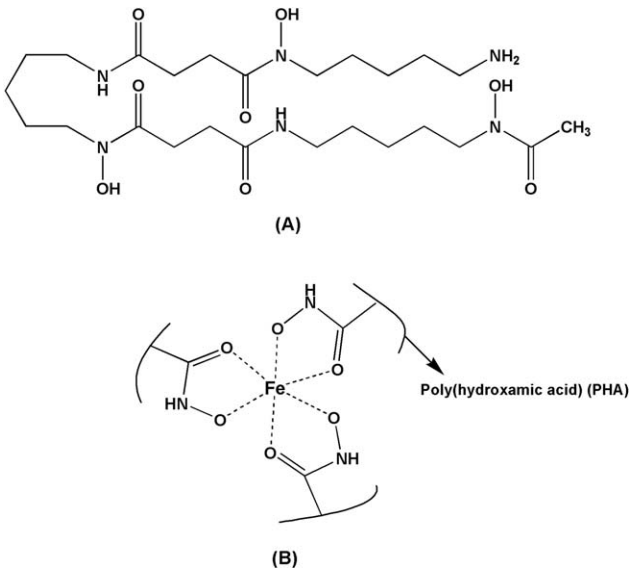


**Figure 1.** Chemical structure of DFO (A) and HA/Fe complex (B).

In this work, we have developed a two-step surface grafting process (Figure 2) to graft the biomimetic metal chelating polymer PHA from the surface of a planar PP solid support. Attenuated total reflectance/Fourier transform infrared (ATR-FTIR) spectroscopy, contact angle, scanning electron microscopy (SEM), and atomic force microscopy (AFM) were used to characterize surface changes before and after the modification. Iron binding kinetics, as well as the influence of pH (3.0, 4.0, and 5.0) on the ability of the film to complex iron was also determined.

## MATERIALS AND METHODS

### Materials

Polypropylene (PP, isotactic, pellets) was purchased from Scientific Polymer Products (Ontario, NY); 2-propanol, acetone, heptane, methanol, sodium acetate trihydrate, ferric chloride anhydrous, hydrochloric acid, trichloroacetic acid (TCA), 4-(2-hydroxyethyl)-1-piperazineethanesulfonic acid (HEPES), acetic acid glacial, water (HPLC grade), and sodium hydroxide were purchased from Fisher Scientific (Fair Lawn, NJ); hydroxylamine hydrochloride, 3-(2-pyridyl)−5,6-diphenyl-1,2,4-triazine-*p,p′*-disulfonic acid disodium salt hydrate (ferrozine, 98+%), and imidazole (99%) were purchased from Acros Organics (Morris Plains, NJ); benzophenone (BP, 99%) and methyl acrylate (MA, 99%) were purchased from Sigma-Aldrich (St. Louis, MO); all the chemicals and solvents were used without further purification.

### Grafting of Poly(hydroxamic acid) (PHA) from PP Solid Support

PP pellets were cleaned in isopropanol two times (10 min per time) by sonication, followed by cleaning in acetone and deionized water using the same procedure sequentially. The cleaned PP pellets were dried in desiccator overnight (25°C, 15% RH), and then pressed into films using a Carver Laboratory Press (160°C, 9000 lbs force; Model B, Fred S. Carver, NJ). PP films with thickness of 225 ± 25 μm were cut into 2 × 2 $cm^2$ pieces and cleaned and dried by the same procedures as PP pellets.

PHA was grafted from the surface of PP film solid supports using a two-step process. In the first step, poly(methyl acrylate) (PMA) was grafted from the PP surface using an adaptation of the photoinitiated graft polymerization technique as reported by Ma et al.[29] and Tian et al.[19] Briefly, 30 μL of BP solution (5 wt % in heptane) was uniformly coated on each side of PP films (2 × 2 $cm^2$) using a spin coater (Model WS-400-6NPP-LITE, Laurell Technologies Corporation, North Wales, PA). BP-coated films were then cut into 1 × 2 $cm^2$ pieces, and each piece was transferred into individual vials with septum-screw caps. The vials were purged with nitrogen for 5 min to remove oxygen, and subjected to ultraviolet (UV) irradiation for 90 s in a Dymax light-curing system (Model 5000 flood, 320–395 nm, 200 mW/$cm^2$, Dymax Corporation, Torrington, CT) to covalently graft BP onto the surface of PP films to obtain PP-BP. PP-BP films were again submerged in individual septum-screw cap vials containing 6 mL of MA monomer solution (70 wt % MA in acetone), followed by purging nitrogen (5 min) to create an oxygen-free reaction environment, and finally 3 min UV

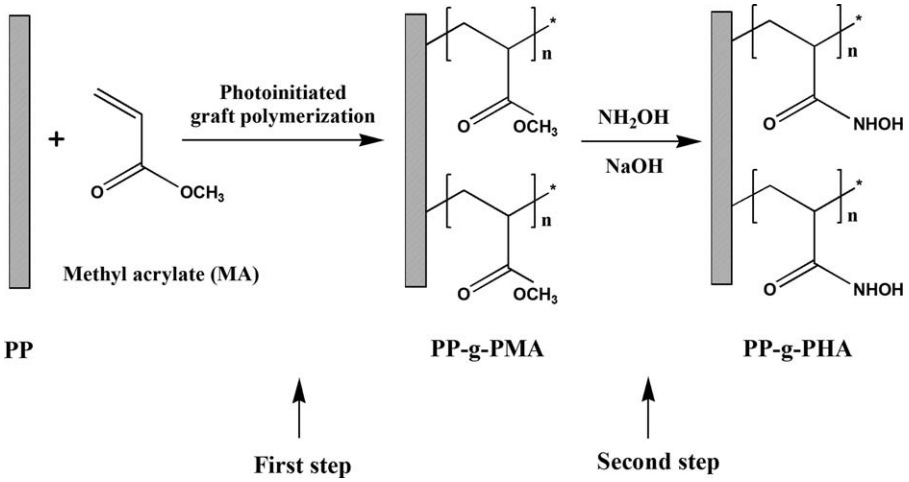


**Figure 2.** Schematic procedure to prepare PP-*g*-PHA films by a two-step surface grafting process.

irradiation. PMA grafted PP (PP-*g*-PMA) films were then washed by Soxhlet extraction in acetone (150 mL) for 12 h to remove the residual MA monomers and non-covalently grafted PMA homopolymers.[30]

In the second step of the PHA grafting procedure, PMA grafts were converted to PHA grafts by a modification of the method reported by Lutfor et al.[5] and Wen et al.[28] Hydroxylamine hydrochloride (20.0 g) was dissolved in 200 mL of methanol/water (5 : 1) solution. The HCl of hydroxylamine hydrochloride was neutralized and the pH of the solution was adjusted to 13 by sodium hydroxide. The generated NaCl precipitate was removed with vacuum filtration to obtain the hydroxylamine reaction solution with the final methanol/water ratio of 4 : 1. PP-*g*-PMA films were submerged in the hydroxylamine solution in a round-bottom flask and allowed to react for 4 h at 73°C with stirring. A reflux condenser was equipped on the flask to maintain the methanol/water ratio during the reaction. After the reaction, films were taken out and rinsed three times in methanol/water (5 : 1) solution to remove the residual hydroxylamine solution. Films were then treated with acidic methanol/water (5 : 1) solution (0.2*M* HCl) for 5 min, followed with rinsing them in methanol/water (5 : 1) solution three times again. Finally, films were washed 3 times (30 min per time) in deionized water to remove any residual compounds from the inner grafting layer. The obtained PP-*g*-PHA films were dried and stored in a desiccator (25°C, 15% RH) until further use.

### Surface Characterization

The surface chemistry of films before and after PHA grafting was analyzed by an IRPrestige-21 FTIR spectrometer (Shimadzu Scientific Instruments, Kyoto, Japan) equipped with a diamond ATR crystal. Each spectrum was done with 32 scans at a 4 $cm^{-1}$ resolution compared with a background spectrum that was done with the ATR crystal against air. Representative spectra of each sample were replotted with SigmaPlot 12.0 (Systat Software, Chicago, IL).

The surface hydrophilicity of films was analyzed by water contact angles carried out on a DSA 100 (Kruss, Hamburg, Germany) equipped with a direct dosing system (DO3210, Kruss, Hamburg, Germany). Water (HPLC grade) was used as the probe liquid to conduct all measurements under ambient conditions. Both advancing and receding angles were recorded every 0.10 s for 18 s and fitted using tangent method-2. The advancing and receding contact angles presented here are the averages of six measurements on three independent films.

The surface and cross-sectional morphologies of films were analyzed by field emission SEM (JEOL 6320 FXV, Japan). Films were sectioned on a cryo-ultramicrotome (−120°C, Leica Microsystems, Germany) equipped with a diamond blade. Samples were sputter-coated (108 sputter coater, Cressington Scientific, UK) with gold for 3 min to prevent charging during SEM analysis.

AFM was performed to quantify the surface topography of films (Dimension-3000 Model with a NanoScope IIIa controller, Digital Instruments, Santa Barbara, CA). Tapping mode images (height and amplitude) of films were collected under ambient conditions using a silicon cantilever tip (uncoated, AppNano ACT-R-W type) with a spring constant of 40 N/m. The scanning area for each sample was 50 × 50 $\mu m^2$, and the average roughness ($R_a$) and the root mean square roughness ($R_{RMS}$) were calculated by the built-in software.

### Iron Chelating Assay

The ferric iron ($Fe^{3+}$) chelating kinetics of PP-*g*-PHA films was determined at pH 5.0, and the effect of pH (3.0, 4.0, and 5.0) on the chelating activity was also quantified. For the iron chelating kinetics study, films (native PP, PP-*g*-PMA, and PP-*g*-PHA; 1 × 2 $cm^2$) were submerged in 0.08 mM $Fe^{3+}$ (from ferric chloride anhydrous) in sodium acetate/imidazole buffer (0.05*M*, pH 5.0), with $Fe^{3+}$ solution without films serving as a control. Films were allowed to chelate in the dark for up to 36 h at room temperature with shaking. The $Fe^{3+}$ chelating activity of films was calculated by the difference of the $Fe^{3+}$ concentration (determined by ferrozine assay, described below) in $Fe^{3+}$ solution with films against the control group ($Fe^{3+}$ solution with no films). To determine the effect of pH on the $Fe^{3+}$ chelating activity of films, $Fe^{3+}$ chelating solutions (0.08 m*M*) with different pH (3.0, 4.0, and 5.0) were prepared using the sodium acetate/imidazole buffer (0.05*M*), and films were allowed to chelate for 24 h.

A modification of the ferrozine assay was performed to quantify the $Fe^{3+}$ concentration of chelating solutions, in which a colorimetric complex is formed between $Fe^{2+}$ and ferrozine reagent.[20,31] First, $Fe^{3+}$ was reduced to $Fe^{2+}$ by exposure to 5 wt % hydroxylamine hydrochloride in 10 wt % TCA. The iron solution (0.5 mL) was mixed with 0.25 mL of reducing agent (5 wt % hydroxylamine hydrochloride, 10 wt % TCA), to which 0.25 mL of ferrozine reagent (18 mM in 0.05 M HEPES buffer, pH 7.0) was added. The absorbance was detected at 562 nm after 1 h of incubation at room temperature with shaking. The $Fe^{3+}$ concentration was quantified by a comparison to a standard curve made of ferric chloride anhydrous. The results are representative of two experiments performed on independent days.

### Statistical Analysis

The data presented are means ± standard deviation (SD) ($n \geq 3$). SPSS Release 17.0 (SPSS, Chicago, IL) was used to conduct the statistical analyses. The significance of variances was assessed by a one-way ANOVA analysis with Duncan's pairwise comparison ($P < 0.05$).

## RESULTS AND DISCUSSION

Photoinitiated graft polymerization is an efficient and economical technique to introduce sufficient amount of functional groups onto inert solid supports by covalent linkages. To the best of our knowledge, there are no commercially available monomers containing HA groups that are suitable for photoinitiated graft polymerization. The commonly used approach to prepare synthetic PHA polymers is by the hydroxylamidation reaction of active moieties including acrylic ester,[5,28] acrylamide,[24,25] acrylonitrile,[32] and acid chloride.[4,17,26] Hence, we herein chose methyl acrylate, which contains an acrylic ester group, as the monomer to covalently graft a high density of acrylic ester active groups from the PP substrate surface in the first step. In

the second step, ester moieties were converted to HA groups by the reaction with hydroxylamine. This two-step surface grafting process is also applicable to prepare biomimetic metal chelating interfaces using other substrate materials (polyolefin films and membranes, etc.).

### Characterization of PHA Grafted PP Films

The surface chemistry of films after each step of modification was measured by the ATR-FTIR analysis (Figure 3). After the grafting of PMA, a strong absorption band appeared at 1740 $cm^{-1}$ compared with the native PP and PP-BP films, which corresponds to the C═O of ester groups of PMA. A medium strong absorption band also was found at 1200 $cm^{-1}$, which is corresponding to the C—O bond of the ester groups. After the conversion of ester groups into HA groups, the absorption bands at 1740 and 1200 $cm^{-1}$ disappeared, and three new absorption bands appeared at 1650, 1545, and 3225 $cm^{-1}$, corresponding to C═O, C—NH, and —OH of HA groups, respectively. The results of ATR-FTIR analysis indicated the successful grafting of PMA, as well as the conversion of ester groups into HA groups.

The advancing and receding water contact angles of PP, PP-*g*-PMA, and PP-*g*-PHA films were measured to quantify the change in surface hydrophilicity of films before and after the grafting procedure (Table I). The native PP film showed a typical hydrophobic surface. Compared with the native PP film, both advancing and receding angles of the PP-*g*-PMA film significantly decreased, showing a less hydrophobic surface. A higher hysteresis was also observed on the PP-*g*-PMA film surface compared to the native PP film. Hysteresis represents the difference between the advancing and the receding angles of a surface, which is related to the surface roughness, surface chemical composition, the interaction between surface components and water, etc.[33,34] The increase of the surface hysteresis of PP-*g*-PMA films might be a result of the introduction of PMA grafting layer, which could cause the increase of surface roughness, as evidenced by the AFM analysis (discussed below). The surface hydrophilicity of films significantly increased after the conversion of PMA into PHA, which is consistent with the highly hydrophilic nature of HA groups.[24] The results of the contact angle analysis further confirmed the successful grafting of PHA from the PP film surface.

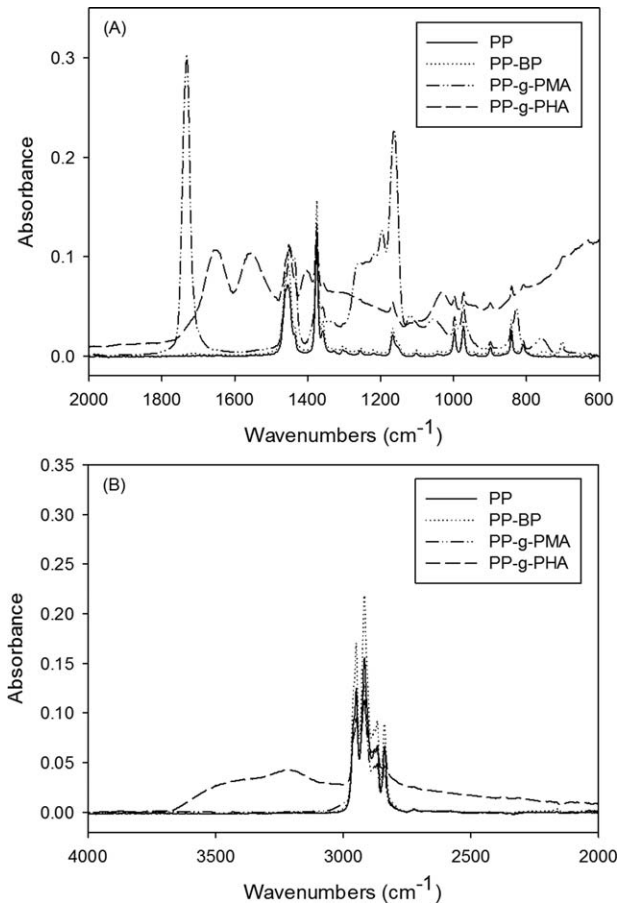


**Figure 3.** ATR-FTIR spectra of native PP, PP-BP, PP-*g*-PMA, and PP-*g*-PHA film surface in the range of 2000–600 $cm^{-1}$ (A) and 4000–2000 $cm^{-1}$ (B).

**Table I.** The Surface Water Contact Angles of PP, PP-*g*-PMA, and PP-*g*-PHA Films

| Contact angle | Advancing (°) | Receding (°) | Hysteresis (°) |
|---|---|---|---|
| PP | $105.9 \pm 1.2^a$ | $87.7 \pm 2.3^a$ | 18.2 |
| PP-*g*-PMA | $75.6 \pm 3.7^b$ | $37.0 \pm 1.6^b$ | 38.6 |
| PP-*g*-PHA | $14.9 \pm 2.4^c$ | $6.6 \pm 0.3^c$ | 8.3 |

Values are averages ± standard deviations ($n = 6$). Different superscript letters in the same column indicate significant differences ($P < 0.05$).

SEM was performed to analyze the surface and cross-sectional morphology of native PP, PP-*g*-PMA, and PP-*g*-PHA films (Figure 4). The surface SEM images of PP, PP-*g*-PMA, and PP-*g*-PHA films presented no clear morphology [Figure 4(A–C)] suggesting a uniform grafting process with no evident defects. Compared to the cross-sectional image of native PP film [Figure 4(D)], two distinct phases were observed in the cross-sectional image of PP-*g*-PMA film [Figure 4(E)], and the left-most phase was identified as the PMA grafting layer resulted from the photoinitiated polymerization of MA monomers. SEM images were taken at three points on cross-sections of two independent films, and the thickness of the PMA grafting layer was determined to be $26 \pm 4$ $\mu$m. In Figure 4(F), three phases with different textures were distinguished on the cross-section of PP-*g*-PHA films, and the total thickness of the two outermost layers was around 25 $\mu$m. These two layers correspond to the PMA (middle layer) and PHA (left layer) grafts, respectively. The interpenetrated interface between the PMA layer and the PP substrate could be a result of the surface grafting process in which some photoinitiator was entrapped into a thin layer of the PP polymer.[35] Conversely, there is a distinct and uniform interface between the PHA and PMA layers, indicating a uniform metal chelating surface. The PHA/PMA thickness ratio (~1 : 2) suggested that the conversion ratio of PMA to PHA was approximately 30%. This conversion rate is comparable to previously reported research in which Crumbliss et al. demonstrated 35% conversion of acyl chloride to HA based on elemental analysis.[36]

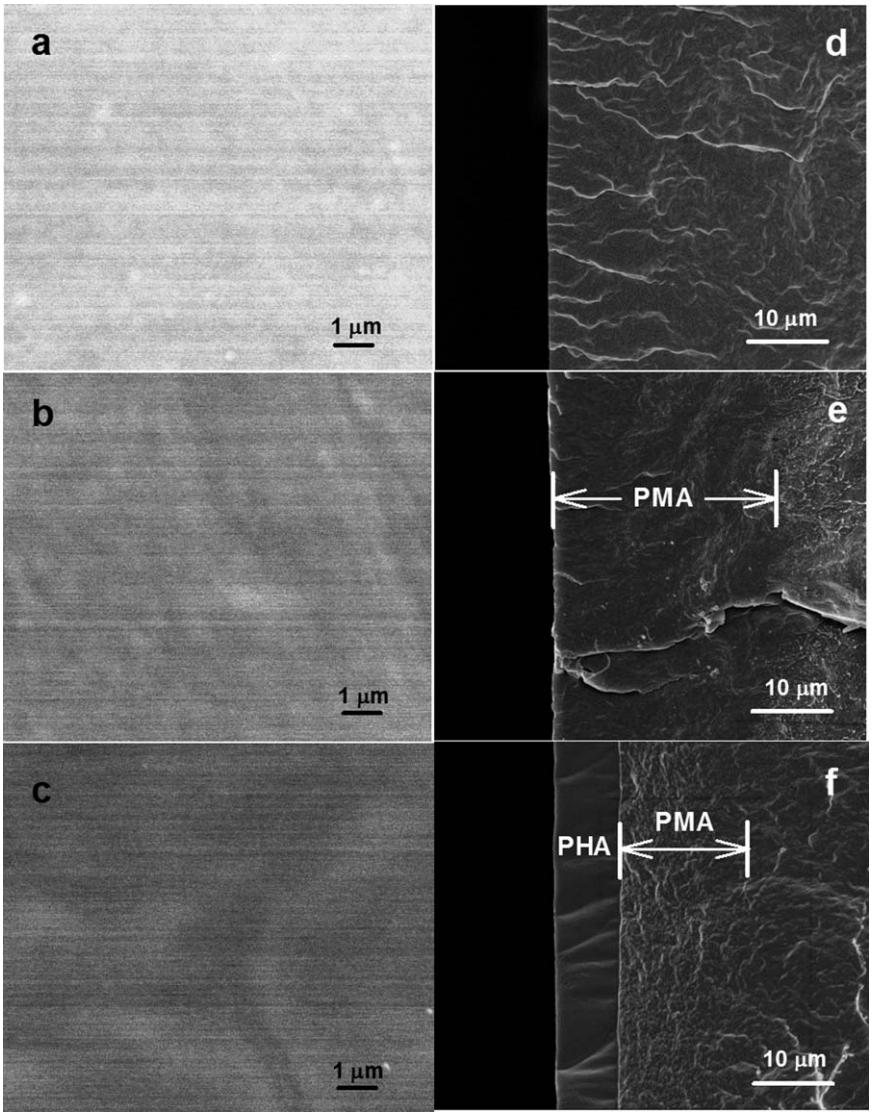


**Figure 4.** Surface and cross-sectional SEM images of PP, PP-*g*-PMA, and PP-*g*-PHA films: (A) surface image of PP film surface; (B) surface image of PP-*g*-PMA film surface; (C) surface image of PP-*g*-PHA film surface; (D) cross-sectional image of PP film surface; (E) cross-sectional image of PP-*g*-PMA film surface; (F) cross-sectional image of PP-*g*-PHA film surface. The images presented here are representative of six images taken on two independent samples.

AFM was used to acquire the amplitude and topography images of films after each step of modification (Figure 5), as well as their surface roughness (Table II). Figure 5(A1–C1) correspond to the amplitude images of native PP, PP-*g*-PMA, and PP-*g*-PHA films, respectively, showing the surface morphology of films. The bare PP substrate presented a relatively featureless surface, in agreement with results from SEM imaging. More features were observed in the AFM amplitude images of PP-*g*-PMA and PP-*g*-PHA films, compared with their SEM surface images [Figure 4(B,C)]. As the imaging was conducted in a dry state (under the ambient condition), the dehydrated grafting chains displayed a collapsed appearance in terms of both modified surfaces. Since the polymer-specific features could not be distinguished, PMA grafting exhibited similar morphology to the PHA grafting. Figure 5(A2–C2) illustrate the surface topography of films, and both the average roughness ($R_a$) and root mean square roughness ($R_{RMS}$) of films were calculated (Table II). $R_a$ and $R_{RMS}$ values suggested a significant increase in roughness after the grafting of PMA, compared to the native PP film. This increase in roughness supports the observed increase in contact angle hysteresis of the surface of PP-*g*-PMA films (Table I). The similar roughness values between PMA and PHA grafted films suggested that the conversion from PMA to PHA did not have great influence on the surface roughness of films.

### Iron Chelating Activity

After being submerged in ferric iron solution for 30 min, PP-*g*-PHA films exhibited a red brown color, characteristic of the complex between HA and ferric iron. The intensity of this color increased with increasing incubation time, reaching equilibrium at about 24 h (Figures 6 and 7). There was no color formed on the surface of native PP and PP-*g*-PMA films, indicating that the color was from the formation of PHA/$Fe^{3+}$ complex, not due to the nonspecific adsorption of iron, polymerized iron, or

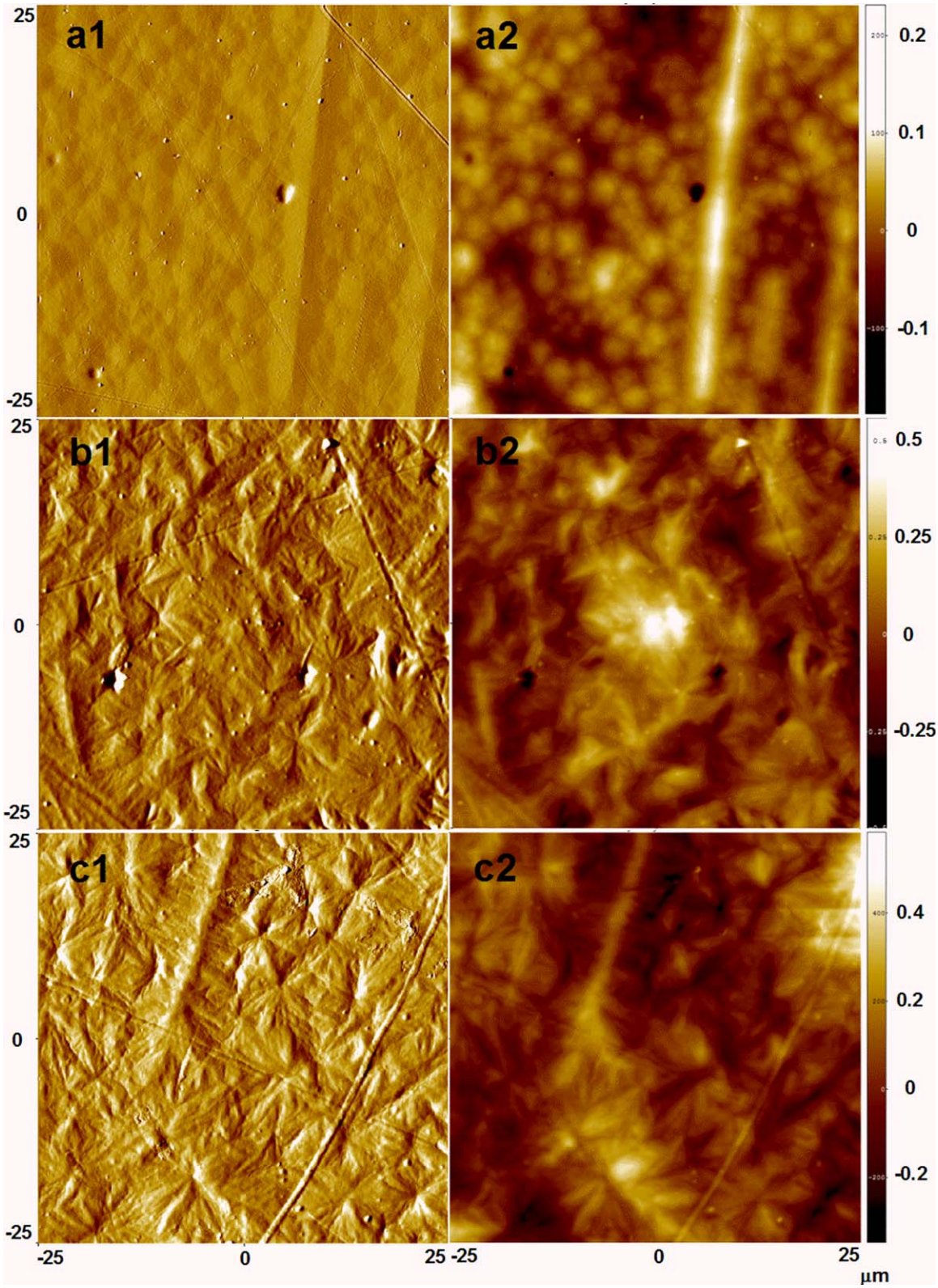


**Figure 5.** AFM tapping mode images of PP, PP-*g*-PMA, and PP-*g*-PHA films: (A1) amplitude image of PP film surface; (A2) height image of PP film surface; (B1) amplitude image of PP-*g*-PMA film surface; (B2) height image of PP-*g*-PMA film surface; (C1) amplitude image of PP-*g*-PHA film surface; (C2) height image of PP-*g*-PHA film surface. The colored bars on the right-hand side are height indicators with the color related to the real height of each scanned point. [Color figure can be viewed in the online issue, which is available at wileyonlinelibrary.com.]

**Table II.** The Surface Average Roughness ($R_a$) and Root Mean Square Roughness ($R_{RMS}$) of PP, PP-*g*-PMA, and PP-*g*-PHA Films

| Surface roughness | $R_a$ (nm) | $R_{RMS}$ (nm) |
|---|---|---|
| PP | 26.8 | 34.4 |
| PP-*g*-PMA | 87.9 | 111.8 |
| PP-*g*-PHA | 95.8 | 120.7 |

ferric hydroxide precipitate. The formation of the color also indicated that HA groups still maintain their activity to chelate iron after being anchored on a solid support. The even distribution of color across the PP-*g*-PHA film surface (Figure 6) further supports that the PHA grafting technique resulted in uniform surface chemistry, which is in agreement with the SEM results [Figure 4(f)].

The iron chelating kinetics of PP, PP-*g*-PMA, and PP-*g*-PHA films was measured as the function of incubation time at pH 5.0 (Figure 7). While PP and PP-*g*-PMA films did not chelate iron over the study, PP-*g*-PHA films exhibited a significant iron chelating activity, reaching ~80 nmol/cm$^2$ at equilibrium. The iron chelating activity of PP-*g*-PHA films increased linearly with the incubation time from 0.5 to 4 h, and then slowly increased until reaching a plateau after 24 h. It has been reported that hexadentate ligands like DFO (with three HA groups as chelating ligands) form the ligands/iron complex by completely concealing the iron surface, which decelerates the equilibrium rate of the chelation reaction.[18] This low rate of equilibrium for HA functional groups to form the HA/$Fe^{3+}$ complex is likely a reason of the relatively long equilibration time (24 h) for PHA to chelate iron. Winston, et al.[26] also reported a time delay up to 5 h for the chelation reaction between PHA free polymers and ferric iron to achieve equilibrium. Similarly, Kamble et al. synthesized a PHA ion-exchange resin and found that a 4 h reaction time was necessary for maximum absorption in the presence of 1 mg/ml ferric iron.[37] The long equilibrium time might also be a result of the steric hindrance effect from the PP substrate preventing the diffusion of iron ions into the inner layer of PHA. Diffusion of metal ions can be significantly influenced by polymer graft yields. Indeed, Roman et al. demonstrated that grafted polymer chain length and chain surface density had a significant effect on iron chelating activity and ligand to metal binding ratio of poly(acrylic acid) (PAA) grafted from PP.[38]

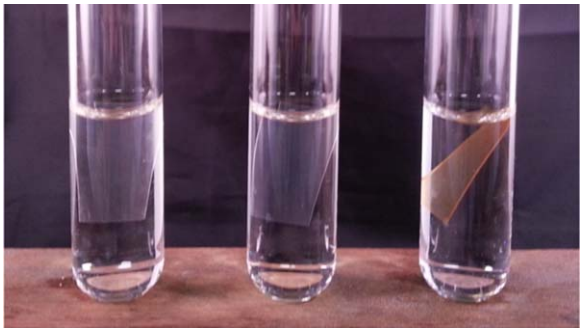

**Figure 6.** The native PP (left), PP-*g*-PMA (middle), and PP-*g*-PHA (right) films after the incubation of 24 h in ferric iron solution (0.08 m*M*, pH 5.0). [Color figure can be viewed in the online issue, which is available at wileyonlinelibrary.com.]

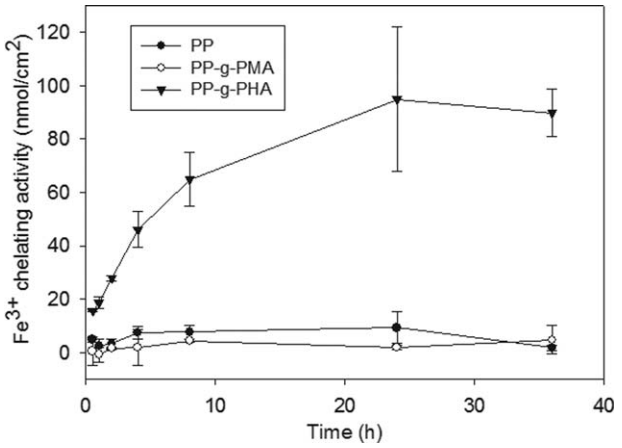


**Figure 7.** Iron chelating activity of native PP, PP-*g*-PMA, and PP-*g*-PHA films with different incubation time in $Fe^{3+}$ solution (0.08 m*M*, pH 5.0).

The ferric iron chelating activity of PP, PP-*g*-PMA, and PP-*g*-PHA films at different pH (3.0, 4.0, and 5.0) was also determined using the equilibration chelating time of 24 h (Figure 8). As iron precipitation was found in the iron chelating solution at pH above 5.0, the activity of films was not detected in the solution with higher pH. While PP and PP-*g*-PMA films did not chelate iron, the PP-*g*-PHA film exhibited strong iron chelating capacity at all tested pHs, and the activity increased with increasing pH. Domb et al.[24] also reported similar results about free PHA molecules. Even though the capacity of metal chelation decreased with decreasing pH, PP-*g*-PHA films were still able to chelate 36.96 ± 4.78 nmol/cm$^2$ iron at pH 3.0, which was approximately 50% of that at pH 5.0. The effect of pH on the iron chelating activity of PHA modified resins and hydrogels has been reported to demonstrate similar trends, wherein >50% activity was maintained when the reaction solution pH was decreased from pH ~5 to ~3.[5,17,28] In prior work, a metal chelating polymer poly(acrylic acid) (PAA) was covalently immobilized onto a LDPE film surface, and the ferric iron chelating activity of this active film (PE-ED-PAA) at pH 3.0 was only around 25% of that at pH 5.0.[20] PAA is a polyelectrolyte with the p*Ka* around 5, and the charge condition of the chelating

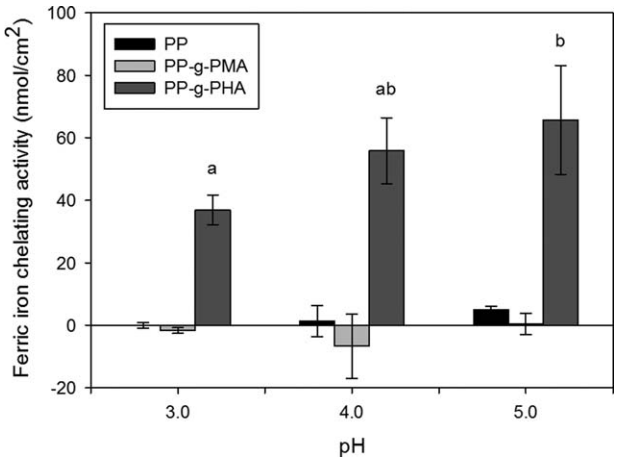


**Figure 8.** Iron chelating activity of native PP, PP-*g*-PMA, and PP-*g*-PHA films at different pH (3.0, 4.0, and 5.0).

ligands (carboxylic acids) has a great impact on its metal chelating activity, which is therefore significantly pH-dependent. The p*Ka* of the metal chelating polymer PHA is ~9, and the predominant species in its aqueous solutions are the protonated HAs at acidic or neutral pH.[39] The charge condition of chelating ligands (HAs) of PHA would not significantly change in the tested pH range (3.0–5.0). HAs allowed metal ions to replace the protons and form the coordination bonds between ligands and metals. The HA-based metal chelators are therefore less sensitive to pH than their carboxylic acid-based counterparts. We have demonstrated that the developed PP-*g*-PHA metal chelating interface has a significant iron chelating activity over a broad active pH range.

## CONCLUSIONS

Siderophore-mimetic metal chelating activity was successfully introduced to the surface of a solid support by photoinitiated grafting PHA from a planar PP substrate. The results of the cross-sectional imaging and the iron complexation reaction demonstrated a uniform PHA grafting layer with a thickness of around 8 $\mu$m. The developed PP-*g*-PHA chelating interface exhibited a strong iron chelating activity (~80 nmol/cm$^2$) with an equilibrium time of 24 h at pH 5.0. At pH 3.0, the PP-*g*-PHA film was able to retain 50% of the ability at pH 5.0 to complex iron, indicating a relatively broad active pH range. The developed surface grafting procedure can also be adapted to prepare biomimetic metal chelating interfaces using other substrate materials (polyolefin films and membranes, etc.). By utilizing siderophore-mimetic surface chemistry, such effective metal chelating interfaces can extend the applications of metal chelating polymers in environmental remediation, water purification, and active packaging areas.

## ACKNOWLEDGMENTS

This work was supported by the United States Department of Agriculture National Institute of Food and Agriculture, and in part by UMass through the CVIP Technology Development Fund, the Peter Salmon Graduate Fellowship (Dept of Food Science, UMass Amherst) and Northeast Alliance Fellowship.

## REFERENCES

1. Bisset, W.; Jacobs, H.; Koshti, N.; Stark, P.; Gopalan, A. *React. Funct. Polym.* **2003**, *55*, 109.
2. Zander, N. E. Army Research Laboratory, *ARL-CR-0623*, **2009**.
3. Ding, P.; Huang, K.; Li, G.; Zeng, W. *J. Hazard. Mater.* **2007**, *146*, 58.
4. Ukey, V.; Juneja, H. *J. Appl. Polym. Sci.* **2006**, *99*, 273.
5. Lutfor, M.; Sidik, S.; Yunus, W.; Rahman, M.; Mansor, A. *J. Appl. Polym. Sci.* **2001**, *79*, 1256.
6. Beauvais, R.; Alexandratos, S. *React. Funct. Polym.* **1998**, *36*, 113.
7. Alakhras, F. A.; Abu Dari, K.; Mubarak, M. S. *J. Appl. Polym. Sci.* **2005**, *97*, 691.
8. Kolodynska, D.; Ning, R. Y., Eds. Expanding Issues in Desalination; InTech, Rijeka, Croatia. **2011**; pp 339.
9. Liu, X.; Hu, Q.; Fang, Z.; Zhang, X.; Zhang, B. *Langmuir* **2009**, *25*, 3.
10. Bukowska, A.; Bukowski, W. *J. Appl. Polym. Sci.* **2012**, *124*, 904.
11. Bessbousse, H.; Verchere, J.; Lebrun, L. *Chem. Eng. J.* **2012**, *187*, 16.
12. Pan, B.; Zhang, W.; Lv, L.; Zhang, Q. *Chem. Eng. J.* **2009**, *151*, 19.
13. Agrawal, Y.; Kaur, H. *Rev. Anal. Chem.* **2001**, *20*, 185.
14. Agrawal, Y. K.; Rao, K. V. *React. Funct. Polym.* **1996**, *31*, 225.
15. Ozkara, S.; zkara, S.; Yavuz, H.; Denizli, A. *J. Appl. Polym. Sci.* **2003**, *89*, 1567.
16. Kenawy, E.; Abdel Hay, F.; El Newehy, M.; Ottenbrite, R. *Polym. Int.* **2008**, *57*, 85.
17. Polomoscanik, S.; Cannon, C.; Neenan, T.; Holmes Farley, S.; Mandeville, W. *Biomacromolecules* **2005**, *6*, 2946.
18. Liu, Z.; Hider, R. *Coord. Chem. Rev.* **2002**, *232*, 151.
19. Tian, F.; Decker, E. A.; Goddard, J. M. *J. Agric. Food Chem.* **2012**, *60*, 7710.
20. Tian, F.; Decker, E. A.; Goddard, J. M. *J. Agric. Food Chem.* **2012**, *60*, 2046.
21. Siebner Freibach, H.; Yariv, S.; Lapides, Y.; Hadar, Y.; Chen, Y. *J. Agric. Food Chem.* **2005**, *53*, 3434.
22. Segura, M.; Madrid, Y.; Camara, C. *J. Anal. At. Spectrom.* **2003**, *18*, 1103.
23. Mohammadi, Z.; Xie, S.; Golub, A.; Gehrke, S.; Berkland, C. *J. Appl. Polym. Sci.* **2011**, *121*, 1384.
24. Domb, A.; Cravalho, E.; Langer, R. *J. Polym. Sci. Part A: Polym. Chem.* **1988**, *26*, 2623.
25. Rosthauser, J.; Winston, A. *Macromolecules* **1981**, *14*, 538.
26. Winston, A.; Kirchner, D. *Macromolecules* **1978**, *11*, 597.
27. Winston, A.; Varaprasad, D.; Metterville, J.; Rosenkrantz, H. *J. Pharmacol. Exp. Ther.* **1985**, *232*, 644.
28. Wen, S. S. Y.; Rahman, M.; Arshad, S.; Surugau, N.; Musta, B. *J. Appl. Polym. Sci.* **2011**, *124*, 4443.
29. Ma, H.; Davis, R.; Bowman, C. *Macromolecules* **2000**, *33*, 331.
30. Abu Ilaiwi, F.; Ahmad, M.; Ibrahim, N.; Ab Rahman, M.; Dahlan, K. *Polym. Int.* **2004**, *53*, 386.
31. Bou, R.; Guardiola, F.; Codony, R.; Faustman, C.; Elias, R.; Decker, E. *J. Agric. Food Chem.* **2008**, *56*, 9612.
32. Vernon, F. *Pure Appl. Chem.* **1982**, *54*, 2151.
33. Gao, L.; McCarthy, T. *Langmuir* **2009**, *25*, 14105.
34. Rangwalla, H.; Schwab, A.; Yurdumakan, B.; Yablon, D.; Yeganeh, M. *Langmuir* **2004**, *20*, 8625.
35. Ulbricht, M.; Yang, H. *Chem. Mater.* **2005**, *17*, 2622.
36. Crumbliss, L; Garrison, J. M; Bock, C. R; Schaaf, A; Bonaventura, C. J; Bonaventura, J. *Inorg. Chem. Acta* **1987**, *133*, 281.
37. Kamble, K. J.; Patkar, D. N. *J. Appl. Polym. Sci.* **1994**, *52*, 1361.
38. Roman, M. J.; Tian, F.; Decker, E. A.; Goddard, J. M. *J. Appl. Polym. Sci.* **2014**, *131*. doi: 10.1002/app.39948.
39. Folkers, J. P.; Gorman, C. B.; Laibinis, P. E.; Buchholz, S.; Whitesides, G. M. *Langmuir* **1995**, *11*, 813.